

PDF hosted at the Radboud Repository of the Radboud University Nijmegen

The following full text is a publisher's version.

For additional information about this publication click this link.

<http://hdl.handle.net/2066/159709>

Please be advised that this information was generated on 2020-09-22 and may be subject to change.

Measurement of the Radiation Energy in the Radio Signal of Extensive Air Showers as a Universal Estimator of Cosmic-Ray Energy

A. Aab,¹ P. Abreu,² M. Aglietta,³ E.J. Ahn,⁴ I. Al Samarai,⁵ I.F.M. Albuquerque,⁶ I. Allekotte,⁷ P. Allison,⁸ A. Almela,^{9,10} J. Alvarez Castillo,¹¹ J. Alvarez-Muñiz,¹² R. Alves Batista,¹³ M. Ambrosio,¹⁴ A. Aminaei,¹⁵ G.A. Anastasi,¹⁶ L. Anchordoqui,¹⁷ S. Andringa,² C. Aramo,¹⁴ F. Arqueros,¹⁸ N. Arsene,¹⁹ H. Asorey,^{7,20} P. Assis,² J. Aublin,²¹ G. Avila,²² N. Awal,²³ A.M. Badescu,²⁴ C. Baus,²⁵ J.J. Beatty,⁸ K.H. Becker,²⁶ J.A. Bellido,²⁷ C. Berat,²⁸ M.E. Bertaina,³ X. Bertou,⁷ P.L. Biermann,²⁹ P. Billoir,²¹ S.G. Blaess,²⁷ A. Blanco,² M. Blanco,²¹ J. Blazek,³⁰ C. Bleve,³¹ H. Blümer,^{25,32} M. Boháčová,³⁰ D. Boncioli,³³ C. Bonifazi,³⁴ N. Borodai,³⁵ J. Brack,³⁶ I. Brancus,³⁷ T. Bretz,³⁸ A. Bridgeman,³² P. Brogueira,² P. Buchholz,¹ A. Bueno,³⁹ S. Buitink,¹⁵ M. Buscemi,¹⁴ K.S. Caballero-Mora,⁴⁰ B. Caccianiga,⁴¹ L. Caccianiga,²¹ M. Candusso,⁴² L. Caramete,⁴³ R. Caruso,¹⁶ A. Castellina,³ G. Cataldi,³¹ L. Cazon,² R. Cester,⁴⁴ A.G. Chavez,⁴⁵ A. Chiavassa,³ J.A. Chinellato,⁴⁶ J. Chudoba,³⁰ M. Cilmo,¹⁴ R.W. Clay,²⁷ G. Cocciolo,³¹ R. Colalillo,¹⁴ A. Coleman,⁴⁷ L. Collica,⁴¹ M.R. Coluccia,³¹ R. Conceição,² F. Contreras,⁴⁸ M.J. Cooper,²⁷ A. Cordier,⁴⁹ S. Coutu,⁴⁷ C.E. Covault,⁵⁰ J. Cronin,⁵¹ R. Dallier,^{52,53} B. Daniel,⁴⁶ S. Dasso,^{54,55} K. Daumiller,³² B.R. Dawson,²⁷ R.M. de Almeida,⁵⁶ S.J. de Jong,^{15,57} G. De Mauro,¹⁵ J.R.T. de Mello Neto,³⁴ I. De Mitri,³¹ J. de Oliveira,⁵⁶ V. de Souza,⁵⁸ L. del Peral,⁵⁹ O. Deligny,⁵ N. Dhital,⁶⁰ C. Di Giulio,⁴² A. Di Matteo,⁶¹ J.C. Diaz,⁶⁰ M.L. Díaz Castro,⁴⁶ F. Diogo,² C. Dobrigkeit,⁴⁶ W. Docters,⁶² J.C. D'Olivo,¹¹ A. Dorofeev,³⁶ Q. Dorosti Hasankiadeh,³² R.C. dos Anjos,⁵⁸ M.T. Dova,⁶³ J. Ebr,³⁰ R. Engel,³² M. Erdmann,³⁸ M. Erfani,¹ C.O. Escobar,^{4,46} J. Espadanal,² A. Etchegoyen,^{10,9} H. Falcke,^{15,64,57} K. Fang,⁵¹ G. Farrar,²³ A.C. Fauth,⁴⁶ N. Fazzini,⁴ A.P. Ferguson,⁵⁰ B. Fick,⁶⁰ J.M. Figueira,¹⁰ A. Filevich,¹⁰ A. Filipčič,^{65,66} O. Fratu,²⁴ M.M. Freire,⁶⁷ T. Fujii,⁵¹ B. García,⁶⁸ D. Garcia-Gamez,⁴⁹ D. Garcia-Pinto,¹⁸ F. Gate,⁵² H. Gemmeke,⁶⁹ A. Gherghel-Lascu,³⁷ P.L. Ghia,²¹ U. Giaccari,³⁴ M. Giammarchi,⁴¹ M. Giller,⁷⁰ D. Glas,⁷⁰ C. Glaser,³⁸ H. Glass,⁴ G. Golup,⁷ M. Gómez Berisso,⁷ P.F. Gómez Vitale,²² N. González,¹⁰ B. Gookin,³⁶ J. Gordon,⁸ A. Gorgi,³ P. Gorham,⁷¹ P. Gouffon,⁶ N. Griffith,⁸ A.F. Grillo,³³ T.D. Grubb,²⁷ F. Guarino,¹⁴ G.P. Guedes,⁷² M.R. Hampel,¹⁰ P. Hansen,⁶³ D. Harari,⁷ T.A. Harrison,²⁷ S. Hartmann,³⁸ J.L. Harton,³⁶ A. Haungs,³² T. Hebbeker,³⁸ D. Heck,³² P. Heimann,¹ A.E. Herve,³² G.C. Hill,²⁷ C. Hojvat,⁴ N. Hollon,⁵¹ E. Holt,³² P. Homola,²⁶ J.R. Hörandel,^{15,57} P. Horvath,⁷³ M. Hrabovský,^{73,30} D. Huber,²⁵ T. Huege,³² A. Insolia,¹⁶ P.G. Isar,⁴³ I. Jandt,²⁶ S. Jansen,^{15,57} C. Jarne,⁶³ J.A. Johnsen,⁷⁴ M. Josebachuili,¹⁰ A. Kääpä,²⁶ O. Kambeitz,²⁵ K.H. Kampert,²⁶ P. Kasper,⁴ I. Katkov,²⁵ B. Keilhauer,³² E. Kemp,⁴⁶ R.M. Kieckhafer,⁶⁰ H.O. Klages,³² M. Kleifges,⁶⁹ J. Kleinfeller,⁴⁸ R. Krause,³⁸ N. Krohm,²⁶ D. Kuempel,³⁸ G. Kukec Mezek,⁶⁶ N. Kunka,⁶⁹ A.W. Kuotb Awad,³² D. LaHurd,⁵⁰ L. Latronico,³ R. Lauer,⁷⁵ M. Lauscher,³⁸ P. Lautridou,⁵² S. Le Coz,²⁸ D. Lebrun,²⁸ P. Lebrun,⁴ M.A. Leigui de Oliveira,⁷⁶ A. Letessier-Selvon,²¹ I. Lhenry-Yvon,⁵ K. Link,²⁵ L. Lopes,² R. López,⁷⁷ A. López Casado,¹² K. Louedec,²⁸ A. Lucero,¹⁰ M. Malacari,²⁷ M. Mallamaci,⁴¹ J. Maller,⁵² D. Mandat,³⁰ P. Mantsch,⁴ A.G. Mariuzzi,⁶³ V. Marin,⁵² I.C. Mariş,³⁹ G. Marsella,³¹ D. Martello,³¹ H. Martinez,⁷⁸ O. Martínez Bravo,⁷⁷ D. Martraire,⁵ J.J. Masías Meza,⁵⁵ H.J. Mathes,³² S. Mathys,²⁶ J. Matthews,⁷⁹ J.A.J. Matthews,⁷⁵ G. Matthiae,⁴² D. Maurizio,⁸⁰ E. Mayotte,⁷⁴ P.O. Mazur,⁴ C. Medina,⁷⁴ G. Medina-Tanco,¹¹ R. Meissner,³⁸ V.B.B. Mello,³⁴ D. Melo,¹⁰ A. Menshikov,⁶⁹ S. Messina,⁶² M.I. Micheletti,⁶⁷ L. Middendorf,³⁸ I.A. Minaya,¹⁸ L. Miramonti,⁴¹ B. Mitrica,³⁷ L. Molina-Bueno,³⁹ S. Mollerach,⁷ F. Montanet,²⁸ C. Morello,³ M. Mostafá,⁴⁷ C.A. Moura,⁷⁶ M.A. Muller,^{46,81} G. Müller,³⁸ S. Müller,³² S. Navas,³⁹ P. Necasal,³⁰ L. Nellen,¹¹ A. Nelles,^{15,57} J. Neuser,²⁶ P.H. Nguyen,²⁷ M. Niculescu-Oglinza,³⁷ M. Niechciol,¹ L. Niemietz,²⁶ T. Niggemann,³⁸ D. Nitz,⁶⁰ D. Nosek,⁸² V. Novotny,⁸² L. Nožka,⁷³ L.A. Núñez,²⁰ L. Ochilo,¹ F. Oikonomou,⁴⁷ A. Olinto,⁵¹ N. Pacheco,⁵⁹ D. Pakk Selmi-Dei,⁴⁶ M. Palatka,³⁰ J. Pallotta,⁸³ P. Papenbreer,²⁶ G. Parente,¹² A. Parra,⁷⁷ T. Paul,^{17,84} M. Pech,³⁰ J. Pękala,³⁵ R. Pelayo,⁸⁵ I.M. Pepe,⁸⁶ L. Perrone,³¹ E. Petermann,⁸⁷ C. Peters,³⁸ S. Petrerá,^{61,88} Y. Petrov,³⁶ J. Phuntsok,⁴⁷ R. Piegaia,⁵⁵ T. Pierog,³² P. Pieroni,⁵⁵ M. Pimenta,² V. Pirronello,¹⁶ M. Platino,¹⁰ M. Plum,³⁸ A. Porcelli,³² C. Porowski,³⁵ R.R. Prado,⁵⁸ P. Privitera,⁵¹ M. Prouza,³⁰ E.J. Quel,⁸³ S. Querschfeld,²⁶ S. Quinn,⁵⁰ J. Rautenberg,²⁶ O. Ravel,⁵² D. Ravignani,¹⁰ D. Reinert,³⁸ B. Revenu,⁵² J. Ridky,³⁰ M. Risse,¹ P. Ristori,⁸³ V. Rizi,⁶¹ W. Rodrigues de Carvalho,¹² J. Rodriguez Rojo,⁴⁸ M.D. Rodríguez-Frías,⁵⁹ D. Rogozin,³² J. Rosado,¹⁸ M. Roth,³² E. Roulet,⁷ A.C. Rovero,⁵⁴ S.J. Saffi,²⁷ A. Saftoiu,³⁷ H. Salazar,⁷⁷ A. Saleh,⁶⁶ F. Salesa Greus,⁴⁷ G. Salina,⁴² J.D. Sanabria Gomez,²⁰ F. Sánchez,¹⁰ P. Sanchez-Lucas,³⁹ E. Santos,⁴⁶ E.M. Santos,⁶ F. Sarazin,⁷⁴ B. Sarkar,²⁶ R. Sarmento,² C. Sarmiento-Cano,²⁰ R. Sato,⁴⁸ C. Scarso,⁴⁸ M. Schauer,²⁶ V. Scherini,³¹ H. Schieler,³² D. Schmidt,³² O. Scholten,^{62,89} H. Schoorlemmer,⁷¹ P. Schovánek,³⁰ F.G. Schröder,³² A. Schulz,³²

J. Schulz,¹⁵ J. Schumacher,³⁸ S.J. Sciutto,⁶³ A. Segreto,⁹⁰ M. Settimo,²¹ A. Shadkam,⁷⁹ R.C. Shellard,⁸⁰ G. Sigl,¹³ O. Sima,¹⁹ A. Śmiałkowski,⁷⁰ R. Šmída,³² G.R. Snow,⁸⁷ P. Sommers,⁴⁷ S. Sonntag,¹ J. Sorokin,²⁷ R. Squartini,⁴⁸ Y.N. Srivastava,⁸⁴ D. Stanca,³⁷ S. Stanič,⁶⁶ J. Stapleton,⁸ J. Stasielak,³⁵ M. Stephan,³⁸ A. Stutz,²⁸ F. Suarez,^{10,9} M. Suarez Durán,²⁰ T. Suomijärvi,⁵ A.D. Supanitsky,⁵⁴ M.S. Sutherland,⁸ J. Swain,⁸⁴ Z. Szadkowski,⁷⁰ O.A. Taborda,⁷ A. Tapia,¹⁰ A. Tepe,¹ V.M. Theodoro,⁴⁶ C. Timmermans,^{57,15} C.J. Todero Peixoto,⁹¹ G. Toma,³⁷ L. Tomankova,³² B. Tomé,² A. Tonachini,⁴⁴ G. Torralba Elipe,¹² D. Torres Machado,³⁴ P. Travnicek,³⁰ M. Trini,⁶⁶ R. Ulrich,³² M. Unger,^{23,32} M. Urban,³⁸ J.F. Valdés Galicia,¹¹ I. Valiño,¹² L. Valore,¹⁴ G. van Aar,¹⁵ P. van Bodegom,²⁷ A.M. van den Berg,⁶² S. van Velzen,¹⁵ A. van Vliet,¹³ E. Varela,⁷⁷ B. Vargas Cárdenas,¹¹ G. Varner,⁷¹ R. Vasquez,³⁴ J.R. Vázquez,¹⁸ R.A. Vázquez,¹² D. Veberič,³² V. Verzi,⁴² J. Vicha,³⁰ M. Videla,¹⁰ L. Villaseñor,⁴⁵ B. Vlcek,⁵⁹ S. Vorobiov,⁶⁶ H. Wahlberg,⁶³ O. Wainberg,^{10,9} D. Walz,³⁸ A.A. Watson,⁹² M. Weber,⁶⁹ K. Weidenhaupt,³⁸ A. Weindl,³² C. Welling,³⁸ F. Werner,²⁵ A. Widom,⁸⁴ L. Wiencke,⁷⁴ H. Wilczyński,³⁵ T. Winchen,²⁶ D. Wittkowski,²⁶ B. Wundheiler,¹⁰ S. Wykes,¹⁵ L. Yang,⁶⁶ T. Yapici,⁶⁰ A. Yushkov,¹ E. Zas,¹² D. Zavrtnik,^{66,65} M. Zavrtnik,^{65,66} A. Zepeda,⁷⁸ B. Zimmermann,⁶⁹ M. Ziolkowski,¹ and F. Zuccarello¹⁶

(The Pierre Auger Collaboration)*

¹ *Universität Siegen, Fachbereich 7 Physik - Experimentelle Teilchenphysik, Siegen, Germany*

² *Laboratório de Instrumentação e Física Experimental de Partículas - LIP and Instituto Superior Técnico - IST, Universidade de Lisboa - UL, Lisboa, Portugal*

³ *Osservatorio Astrofisico di Torino (INAF), Università di Torino and Sezione INFN, Torino, Italy*

⁴ *Fermilab, Batavia, IL, USA*

⁵ *Institut de Physique Nucléaire d'Orsay (IPNO), Université Paris 11, CNRS-IN2P3, Orsay, France*

⁶ *Universidade de São Paulo, Instituto de Física, São Paulo, SP, Brazil*

⁷ *Centro Atómico Bariloche and Instituto Balseiro (CNEA-UNCuyo-CONICET), San Carlos de Bariloche, Argentina*

⁸ *Ohio State University, Columbus, OH, USA*

⁹ *Universidad Tecnológica Nacional - Facultad Regional Buenos Aires, Buenos Aires, Argentina*

¹⁰ *Instituto de Tecnologías en Detección y Astropartículas (CNEA, CONICET, UNSAM), Buenos Aires, Argentina*

¹¹ *Universidad Nacional Autónoma de México, México, D.F., México*

¹² *Universidad de Santiago de Compostela, Santiago de Compostela, Spain*

¹³ *Universität Hamburg, II. Institut für Theoretische Physik, Hamburg, Germany*

¹⁴ *Università di Napoli "Federico II" and Sezione INFN, Napoli, Italy*

¹⁵ *IMAPP, Radboud University Nijmegen, Nijmegen, Netherlands*

¹⁶ *Università di Catania and Sezione INFN, Catania, Italy*

¹⁷ *Department of Physics and Astronomy, Lehman College, City University of New York, Bronx, NY, USA*

¹⁸ *Universidad Complutense de Madrid, Madrid, Spain*

¹⁹ *University of Bucharest, Physics Department, Bucharest, Romania*

²⁰ *Universidad Industrial de Santander, Bucaramanga, Colombia*

²¹ *Laboratoire de Physique Nucléaire et de Hautes Energies (LPNHE),*

Universités Paris 6 et Paris 7, CNRS-IN2P3, Paris, France

²² *Observatorio Pierre Auger and Comisión Nacional de Energía Atómica, Malargüe, Argentina*

²³ *New York University, New York, NY, USA*

²⁴ *University Politehnica of Bucharest, Bucharest, Romania*

²⁵ *Karlsruhe Institute of Technology, Institut für Experimentelle Kernphysik (IEKP), Karlsruhe, Germany*

²⁶ *Bergische Universität Wuppertal, Fachbereich C - Physik, Wuppertal, Germany*

²⁷ *University of Adelaide, Adelaide, S.A., Australia*

²⁸ *Laboratoire de Physique Subatomique et de Cosmologie (LPSC),*

Université Grenoble-Alpes, CNRS/IN2P3, Grenoble, France

²⁹ *Max-Planck-Institut für Radioastronomie, Bonn, Germany*

³⁰ *Institute of Physics of the Academy of Sciences of the Czech Republic, Prague, Czech Republic*

³¹ *Dipartimento di Matematica e Fisica "E. De Giorgi" dell'Università del Salento and Sezione INFN, Lecce, Italy*

³² *Karlsruhe Institute of Technology, Institut für Kernphysik, Karlsruhe, Germany*

³³ *INFN, Laboratori Nazionali del Gran Sasso, Assergi (L'Aquila), Italy*

³⁴ *Universidade Federal do Rio de Janeiro, Instituto de Física, Rio de Janeiro, RJ, Brazil*

³⁵ *Institute of Nuclear Physics PAN, Krakow, Poland*

³⁶ *Colorado State University, Fort Collins, CO, USA*

³⁷ *"Horia Hulubei" National Institute for Physics and Nuclear Engineering, Bucharest-Magurele, Romania*

³⁸ *RWTH Aachen University, III. Physikalisches Institut A, Aachen, Germany*

³⁹ *Universidad de Granada and C.A.F.P.E., Granada, Spain*

⁴⁰ *Universidad Autónoma de Chiapas, Tuxtla Gutiérrez, Chiapas, México*

⁴¹ *Università di Milano and Sezione INFN, Milan, Italy*

⁴² *Università di Roma II "Tor Vergata" and Sezione INFN, Roma, Italy*

- ⁴³*Institute of Space Science, Bucharest-Magurele, Romania*
- ⁴⁴*Università di Torino and Sezione INFN, Torino, Italy*
- ⁴⁵*Universidad Michoacana de San Nicolás de Hidalgo, Morelia, Michoacán, México*
- ⁴⁶*Universidade Estadual de Campinas, IFGW, Campinas, SP, Brazil*
- ⁴⁷*Pennsylvania State University, University Park, PA, USA*
- ⁴⁸*Observatorio Pierre Auger, Malargüe, Argentina*
- ⁴⁹*Laboratoire de l'Accélérateur Linéaire (LAL), Université Paris 11, CNRS-IN2P3, Orsay, France*
- ⁵⁰*Case Western Reserve University, Cleveland, OH, USA*
- ⁵¹*University of Chicago, Enrico Fermi Institute, Chicago, IL, USA*
- ⁵²*SUBATECH, École des Mines de Nantes, CNRS-IN2P3, Université de Nantes, Nantes, France*
- ⁵³*Station de Radioastronomie de Nançay, Observatoire de Paris, CNRS/INSU, Nançay, France*
- ⁵⁴*Instituto de Astronomía y Física del Espacio (IAFE, CONICET-UBA), Buenos Aires, Argentina*
- ⁵⁵*Departamento de Física, FCEyN, Universidad de Buenos Aires and CONICET, Buenos Aires, Argentina*
- ⁵⁶*Universidade Federal Fluminense, EEIMVR, Volta Redonda, RJ, Brazil*
- ⁵⁷*Nikhef, Science Park, Amsterdam, Netherlands*
- ⁵⁸*Universidade de São Paulo, Instituto de Física de São Carlos, São Carlos, SP, Brazil*
- ⁵⁹*Universidad de Alcalá, Alcalá de Henares, Madrid, Spain*
- ⁶⁰*Michigan Technological University, Houghton, MI, USA*
- ⁶¹*Dipartimento di Scienze Fisiche e Chimiche dell'Università dell'Aquila and INFN, L'Aquila, Italy*
- ⁶²*KVI - Center for Advanced Radiation Technology, University of Groningen, Groningen, Netherlands*
- ⁶³*IFLP, Universidad Nacional de La Plata and CONICET, La Plata, Argentina*
- ⁶⁴*ASTRON, Dwingeloo, Netherlands*
- ⁶⁵*Experimental Particle Physics Department, J. Stefan Institute, Ljubljana, Slovenia*
- ⁶⁶*Laboratory for Astroparticle Physics, University of Nova Gorica, Nova Gorica, Slovenia*
- ⁶⁷*Instituto de Física de Rosario (IFIR) - CONICET/U.N.R. and Facultad de Ciencias Bioquímicas y Farmacéuticas U.N.R., Rosario, Argentina*
- ⁶⁸*Instituto de Tecnologías en Detección y Astropartículas (CNEA, CONICET, UNSAM), and Universidad Tecnológica Nacional - Facultad Regional Mendoza (CONICET/CNEA), Mendoza, Argentina*
- ⁶⁹*Karlsruhe Institute of Technology, Institut für Prozessdatenverarbeitung und Elektronik, Karlsruhe, Germany*
- ⁷⁰*University of Łódź, Łódź, Poland*
- ⁷¹*University of Hawaii, Honolulu, HI, USA*
- ⁷²*Universidade Estadual de Feira de Santana, Feira de Santana, Brazil*
- ⁷³*Palacky University, RCPTM, Olomouc, Czech Republic*
- ⁷⁴*Colorado School of Mines, Golden, CO, USA*
- ⁷⁵*University of New Mexico, Albuquerque, NM, USA*
- ⁷⁶*Universidade Federal do ABC, Santo André, SP, Brazil*
- ⁷⁷*Benemérita Universidad Autónoma de Puebla, Puebla, México*
- ⁷⁸*Centro de Investigación y de Estudios Avanzados del IPN (CINVESTAV), México, D.F., México*
- ⁷⁹*Louisiana State University, Baton Rouge, LA, USA*
- ⁸⁰*Centro Brasileiro de Pesquisas Físicas, Rio de Janeiro, RJ, Brazil*
- ⁸¹*Universidade Federal de Pelotas, Pelotas, RS, Brazil*
- ⁸²*Charles University, Faculty of Mathematics and Physics, Institute of Particle and Nuclear Physics, Prague, Czech Republic*
- ⁸³*Centro de Investigaciones en Láseres y Aplicaciones, CITEDEF and CONICET, Villa Martelli, Argentina*
- ⁸⁴*Northeastern University, Boston, MA, USA*
- ⁸⁵*Unidad Profesional Interdisciplinaria en Ingeniería y Tecnologías Avanzadas del Instituto Politécnico Nacional (UPIITA- IPN), México, D.F., México*
- ⁸⁶*Universidade Federal da Bahia, Salvador, BA, Brazil*
- ⁸⁷*University of Nebraska, Lincoln, NE, USA*
- ⁸⁸*Gran Sasso Science Institute (INFN), L'Aquila, Italy*
- ⁸⁹*Vrije Universiteit Brussel, Brussels, Belgium*
- ⁹⁰*Istituto di Astrofisica Spaziale e Fisica Cosmica di Palermo (INAF), Palermo, Italy*
- ⁹¹*Universidade de São Paulo, Escola de Engenharia de Lorena, Lorena, SP, Brazil*
- ⁹²*School of Physics and Astronomy, University of Leeds, Leeds, United Kingdom*

We measure the energy emitted by extensive air showers in the form of radio emission in the frequency range from 30 to 80 MHz. Exploiting the accurate energy scale of the Pierre Auger Observatory, we obtain a *radiation energy* of 15.8 ± 0.7 (stat) ± 6.7 (sys) MeV for cosmic rays with an energy of 1 EeV arriving perpendicularly to a geomagnetic field of 0.24 G, scaling quadratically with the cosmic-ray energy. A comparison with predictions from state-of-the-art first-principle calculations shows agreement with our measurement. The radiation energy provides direct access to the calorimetric energy in the electromagnetic cascade of extensive air showers. Comparison with our

result thus allows the direct calibration of any cosmic-ray radio detector against the well-established energy scale of the Pierre Auger Observatory.

In this work, we address one of the most important challenges in cosmic-ray physics: the accurate determination of the absolute energy scale of cosmic rays. Measurements with surface particle detector arrays rely on assumptions about cosmic-ray composition and on extrapolations of our knowledge about hadronic interactions to energies beyond the reach of the Large Hadron Collider. Consequently, their determination of the absolute cosmic-ray energy suffers from significant uncertainties [1]. Fluorescence detectors measure the calorimetric energy in the electromagnetic cascade of air showers, which allows an accurate determination of the energy of the primary particle [2]. However, fluorescence light detection is only possible at sites with good atmospheric conditions, and precise quantification of scattering and absorption of fluorescence light under changing atmospheric conditions requires extensive atmospheric monitoring efforts [3–6].

An attractive option to determine the energy scale of cosmic-ray particles is given by the detection of radio signals. Radio detection of extensive air showers can be performed at any site not overwhelmed by anthropogenic radio signals, requiring only detector arrays of moderate size and complexity. It has been known since the 1960s that air showers emit measurable radio pulses [7]. The physics of the radio emission from extensive air showers is by now well understood (see [8] for an overview). The radiation dominantly arises from geomagnetically induced, time-varying transverse currents [9, 10] and is strongly forward beamed in a cone of a few degree opening angle due to the relativistic speed of the emitting particles. The atmosphere is transparent for radio waves at the relevant frequencies, i.e., scattering and absorption are negligible. As the emission is generally coherent at frequencies below 100 MHz, the amplitude of the electric field scales linearly with the number of electrons and positrons in the air-shower cascade, which in turn scales linearly with the primary cosmic-ray energy.

Several analyses exploiting this calorimetric property of the radio emission for the determination of the energy of cosmic-ray particles have previously been published [11–14]. All of these approaches used the radio-signal strength at a characteristic lateral distance from the shower axis as an estimator for the cosmic-ray energy. While this method has long been known to provide good precision [15], it has the marked disadvantage that the corresponding energy estimator cannot be directly compared across different experiments. Asymmetries arising from the charge-excess contribution [16–18] can be corrected for, and the air-shower zenith angle can be normalized out. The systematic influence of the observation altitude on the lateral signal distribution, however, poses a fundamental problem for such comparisons. In

a simulation study, we have quantified the difference between radio amplitudes at the characteristic lateral distance measured for the same showers at sea level (altitude of LOFAR [19]) and at 1560 m above sea level (altitude of the radio detector array of the Pierre Auger Observatory [20]). We observe differences between -11% and +23% with an average deviation of 11%. These deviations in the measured amplitude arise from the fact that the lateral radio signal distribution flattens systematically with increasing distance of the radio antennas to the air-shower maximum. Furthermore, the optimal lateral distance at which to make the measurement also varies with observation altitude [21]. While absolute values for the amplitudes measured at a characteristic lateral distance as a function of cosmic-ray energy have been published by several experiments [13, 14, 22], no direct comparison between the energy scales of these cosmic-ray radio detectors has therefore been performed to date. (Most experiments obtain their energy scale based on surface detector arrays and thus incur uncertainties from hadronic interaction models.)

Here, we make an important conceptual step forward in using radio signals from extensive air showers for the absolute calibration of the energy scale of cosmic-ray detectors. We use the total energy radiated by extensive air showers in the form of radio emission in the frequency range from 30 to 80 MHz, hereafter called *radiation energy*, as an estimator of the cosmic-ray energy. Due to conservation of energy, and the absence of absorption in the atmosphere, the radiation energy measured at different observation altitudes is virtually identical. In the above-mentioned simulation study, the radiation energy was shown to vary less than 0.5% between an observation altitude of 1560 m above sea level and sea level itself. (This scatter arises from slight clipping effects of the air-shower evolution at an observation altitude of 1560 m above sea level and from statistical uncertainties in the determination of the radiation energy from the simulated radio-emission footprint.) The radiation energy directly reflects the calorimetric energy in the electromagnetic cascade of an extensive air shower, akin to an integral of the Gaisser-Hillas profile measured with fluorescence detectors. It constitutes a universal, well-defined quantity that can be measured with radio detectors worldwide and can thus be compared directly between different experiments, as well as with theoretical predictions.

In this work, we measure the absolute value of the radiation energy with the Auger Engineering Radio Array (AERA) [23], an array of radio detectors in the Pierre Auger Observatory [20]. We then cross-calibrate our measurement with data taken with the baseline detectors of the Auger Observatory. The Observatory includes

an array of water-Cherenkov particle detectors covering an area of 3,000 km². The atmosphere above the surface detector is monitored by fluorescence telescopes which provide an absolute calibration of the cosmic-ray energy scale [24] with a systematic uncertainty of 16% at 10^{17.5} eV and 14% at energies $\geq 10^{18}$ eV [2], reflecting the state-of-the-art in the determination of the absolute energy scale achieved to date. We thus use the accurate calibration of the energy scale of the Pierre Auger Observatory to relate the radiation energy to the cosmic-ray energy. The radiation energy can in turn be used to calibrate cosmic-ray radio detectors worldwide against the Auger energy scale. Finally, we provide a first comparison with predictions from first-principle calculations.

Details of the analysis presented here can be found in an accompanying publication [25].

The energy content in the radio signal.—With the radio antennas of AERA, we continuously sample voltage traces arising from the measurement of the local electric field with antennas oriented along the geomagnetic north-south and east-west directions. Upon a trigger from coincident radio pulses or external trigger information from other Auger detectors, the voltage traces are read out for off-line analysis [26]. From these voltage traces, we reconstruct the electric field vector at the location of each radio detector as a function of time. Detector effects are carefully unfolded [25]. The uncertainty of the electric field amplitude between different measurements is dominated by temperature variations (4%) and uncertainties of the antenna response pattern (5%), and amounts to a total of 6.4%. The uncertainty of the absolute amplitude scale is dominated by the antenna response (12.5% [22, 27]) and the analog signal chain (6%) and amounts to a total of 14%.

After digital processing (involving noise cleaning, up-sampling and enveloping), we identify radio pulses exceeding a suitable signal-to-noise threshold. We calculate the instantaneous Poynting flux at each radio detector and integrate it over a time window of 200 ns which is centered on the pulse maximum. The contribution of noise to the integral is estimated from data recorded before the arrival of the extensive air shower, and is subtracted from the integrated signal. The result of the time-integration corresponds to the energy deposited per area by air-shower radio signals at the locations of the individual radio detectors. We measure this *energy fluence* in units of eV/m². Typical values are in the range of dozens of eV/m². The energy of a photon at our center-of-band frequency of 55 MHz corresponds to 2.27×10^{-7} eV. The number of received photons is thus very high, illustrating that uncertainties from photon statistics are negligible in radio detection of extensive air showers.

The area illuminated by radio signals has a limited extent due to the forward-beamed nature of the radio emission. The local energy fluence at the radio detectors with an identified signal is fitted with a two-dimensional

distribution function of the signal [28], adapted to the observation altitude of AERA, which takes into account azimuthal asymmetries arising from the superposition of geomagnetic and charge-excess [16–18] effects as well as ring-shaped areas of enhanced emission caused by Cherenkov-like time compression due to the refractive index in the atmosphere [29, 30]. During the fit procedure, spurious radio pulses not related to the extensive air shower are flagged and rejected by means of the signal polarization. In rare cases, flagging of spurious radio pulses can lead to rejection of a complete event. An example for the resulting fit is illustrated in Fig. 1. For radio events detected in three or four radio detectors, the impact point of the shower axis used for the fit is fixed to the one reconstructed with the Auger surface detector. For radio events with signals in five or more radio detectors, the impact point is determined during the fit of the two-dimensional signal distribution function.

After a successful fit of the signal distribution function we analytically integrate it over the plane perpendicular to the shower axis. The result is the total energy measured in the radio signal $E_{30-80\text{MHz}}^{\text{Auger}}$ (in units of eV), the *radiation energy*. This quantity does not depend on any characteristics of the detector except the finite measurement bandwidth from 30 to 80 MHz. The superscript “Auger” emphasizes that this quantity applies to the geomagnetic field strength as present at the site of the Pierre Auger Observatory in southern Argentina.

Cross-calibration with the Auger energy scale.—To establish the relation between the radiation energy and the absolute energy scale of cosmic rays, we analyzed data from the first stage of AERA taken between April 2011 and March 2013, when the array consisted of 24 radio detectors equipped with logarithmic-periodic dipole antennas [27]. The signal distribution fit was applied to data pre-selected with standard Auger quality cuts for surface detector events measured with the 750 m grid of the array. We allowed a maximum zenith angle of 55° and required an energy of at least 10¹⁷ eV. This resulted in a data set with 126 events.

For each of these events, the cosmic-ray energy E_{CR} as reconstructed with the Auger surface detector [31] is available. We stress that the energy reconstruction of the surface detector has been calibrated with the calorimetric energy measurement of the fluorescence detector using a subset of events measured with both detectors simultaneously. Due to the dominance of geomagnetic radio emission [11, 18, 32] and the scaling of its amplitude with the magnitude of the Lorentz force, the radiation energy scales with $\sin^2(\alpha)$, where α denotes the angle between the air-shower axis and the geomagnetic-field axis. We thus normalize the radiation energy for perpendicular incidence with respect to the geomagnetic field by dividing it by $\sin^2(\alpha)$. This normalization is valid for all incoming directions of cosmic rays except for a small region around the geomagnetic-field axis. In particular, it is valid for

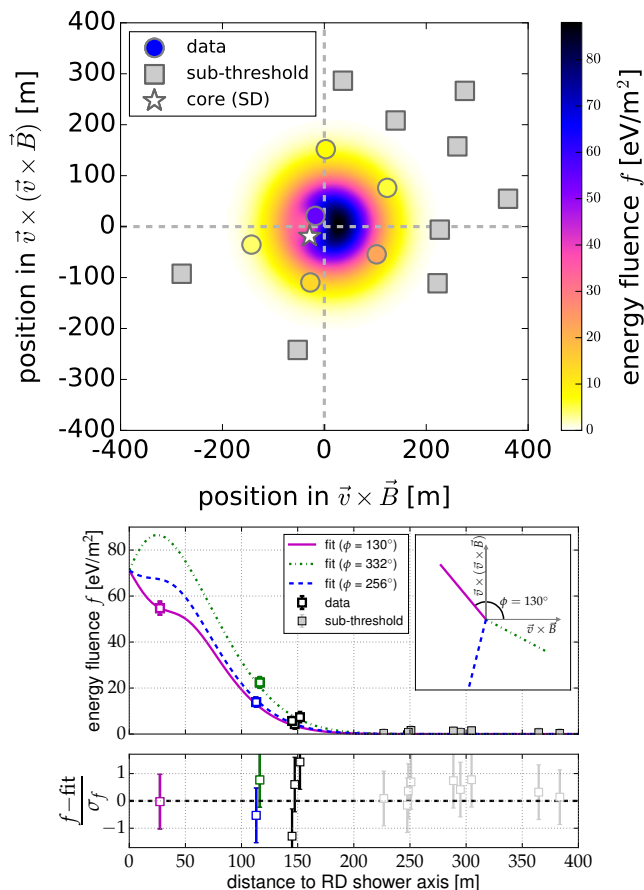


FIG. 1. Top: Energy fluence for an extensive air shower with an energy of 4.4×10^{17} eV, and a zenith angle of 25° as measured in individual AERA radio detectors (circles filled with color corresponding to the measured value) and fitted with the azimuthally asymmetric, two-dimensional signal distribution function (background color). Both, radio detectors with a detected signal (*data*) and below detection threshold (*sub-threshold*) participate in the fit. The fit is performed in the plane perpendicular to the shower axis, with the x -axis oriented along the direction of the Lorentz force for charged particles propagating along the shower axis \vec{v} in the geomagnetic field \vec{B} . The best-fitting impact point of the air shower is at the origin of the plot, slightly offset from the one reconstructed with the Auger surface detector (*core (SD)*). Bottom: Representation of the same data and fitted two-dimensional signal distribution as a function of distance from the shower axis. The colored and black squares denote the energy fluence measurements, gray squares represent radio detectors with signal below threshold. For the three data points with the highest energy fluence, the one-dimensional projection of the two-dimensional signal distribution fit onto lines connecting the best-fitting impact point of the air shower with the corresponding radio detector positions is illustrated with colored lines. This demonstrates the azimuthal asymmetry and complexity of the two-dimensional signal distribution function. The inset figure illustrates the polar angles of the three projections. The distribution of the residuals (data versus fit) is shown as well.

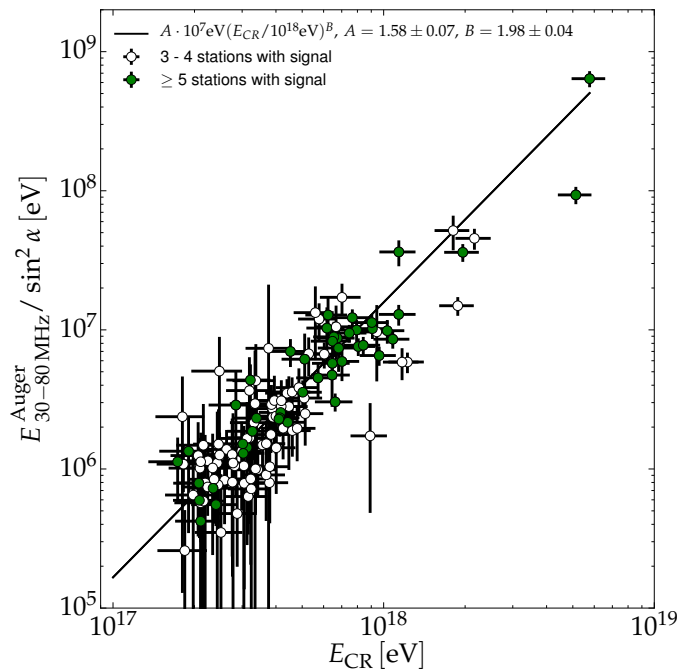


FIG. 2. Correlation between the normalized radiation energy and the cosmic-ray energy E_{CR} as determined by the Auger surface detector. Open circles represent air showers with radio signals detected in three or four radio detectors. Filled circles denote showers with five or more detected radio signals.

all events in the data set presented here.

In Fig. 2, the value of $E_{30-80 \text{ MHz}}^{\text{Auger}} / \sin^2(\alpha)$ for each measured air shower is plotted as a function of the cosmic-ray energy measured with the Auger surface detector. A log-likelihood fit taking into account threshold effects, measurement uncertainties and the steeply falling cosmic-ray energy spectrum [33] shows that the data can be described well with the power law

$$E_{30-80 \text{ MHz}}^{\text{Auger}} / \sin^2(\alpha) = A \times 10^7 \text{ eV} (E_{\text{CR}} / 10^{18} \text{ eV})^B. \quad (1)$$

The result of the fit yields $A = 1.58 \pm 0.07$ and $B = 1.98 \pm 0.04$. For a cosmic ray with an energy of 1 EeV arriving perpendicularly to the Earth's magnetic field at the Pierre Auger Observatory, the radiation energy thus amounts to 15.8 MeV, a minute fraction of the energy of the primary particle. The observed quadratic scaling is expected for coherent radio emission, for which amplitudes scale linearly and thus the radiated energy scales quadratically.

Taking into account the energy- and zenith-dependent uncertainty of E_{CR} , the resolution of $E_{30-80 \text{ MHz}}^{\text{Auger}} / \sin^2(\alpha)$ is determined from the scatter of points in Fig. 2. It amounts to 22% for the full data set. Performing this analysis for the high-quality subset of events with a successful radio detection in at least five radio detectors yields a resolution of 17%.

The value of A reported here applies for a cosmic-ray

shower with an energy of 1 EeV evolving in a geomagnetic field with a strength of 0.24 G, as present at the site of the Pierre Auger Observatory. With dedicated simulations we confirmed that the radiation energy is only marginally influenced by the charge-excess contribution (at the level of 2% for showers arriving perpendicular to the magnetic field at the Pierre Auger site, less for stronger geomagnetic fields). Hence, a normalization with the field strength of the geomagnetic field is possible and yields:

$$E_{30-80\text{MHz}} = (15.8 \pm 0.7 \text{ (stat)} \pm 6.7 \text{ (sys)}) \text{ MeV} \\ \times \left(\sin \alpha \frac{E_{\text{CR}}}{10^{18} \text{ eV}} \frac{B_{\text{Earth}}}{0.24 \text{ G}} \right)^2. \quad (2)$$

$E_{30-80\text{MHz}}$ can be used by radio detectors worldwide for cross-calibration of the energy scale, except for experiments deployed at high altitude where part of the radio emission is clipped when the shower reaches the ground before radiating the bulk of its radio emission. The frequency window from ~ 30 to ~ 80 MHz is shared by many radio detectors [11, 34–36]: below 30 MHz atmospheric noise and transmitters in the short-wave band dominate, above 80 MHz coherence diminishes and the FM-band interferes with the measurement. Possible second-order effects arising in the determination of $E_{30-80\text{MHz}}$, e.g., due to shower geometry, should be addressed in a follow-up analysis because they could lead to further improvements. The systematic uncertainty of $E_{30-80\text{MHz}}$ quoted here arises from the quadratic sum of the systematic uncertainty on the energy scale of the Pierre Auger Observatory (16% at $10^{17.5}$ eV, propagated from the fluorescence detector to the surface detector) and the uncertainty on the radio-electric field amplitude measurement (14%). These two contributions amount to uncertainties of 5.1 and 4.4 MeV in the measurement of the radiation energy at 1 EeV, respectively. We note that the systematic uncertainty in the determination of the cosmic-ray energy from radio measurements is half of that of $E_{30-80\text{MHz}}$, as the cosmic-ray energy scales with the square root of the radiation energy.

Comparison with first-principle calculations.—In addition to a *cross-calibration* of techniques and experiments against each other, the radiation energy can also be used for an *independent determination* of the absolute energy scale of cosmic-ray observatories. Sophisticated Monte Carlo simulations [30, 37, 38] provide a quantitative prediction of the radiation energy based on first-principle calculations combining classical electrodynamics with the well-established properties of the electromagnetic cascade in extensive air showers. A direct comparison of the predicted and measured radiation energies can thus be used for an absolute determination of the energy scale of cosmic-ray detectors.

We have evaluated the radiation energy at a cosmic-ray energy of 1 EeV using the typical zenith angle of our event

sample of 37° and a geomagnetic field strength of 0.24 G with the two available full Monte Carlo simulation codes CoREAS [37] and ZHAireS [30]. The predicted values for the radiation energy amount to 11.9 MeV and 11.3 MeV, respectively. Both predictions are thus in agreement with our measurement within the quoted uncertainties. Further work will be undertaken to better understand and minimize experimental and theoretical systematic uncertainties.

Conclusions.—We have measured the *radiation energy* of extensive air showers and have used it as an energy estimator directly reflecting the calorimetric energy in the electromagnetic cascade. Its value is $15.8 \pm 0.7 \text{ (stat)} \pm 6.7 \text{ (sys)} \text{ MeV}$ in the frequency band from 30 to 80 MHz for a cosmic ray with an energy of 10^{18} eV arriving perpendicularly to a magnetic field with a strength of 0.24 G. The radiation energy can be measured at any location that does not suffer from strong anthropogenic noise using moderately sized radio detector arrays. It can thus be used for an efficient cross-calibration of the energy scales of different experiments and detection techniques against each other, in particular against the well-established energy scale of the Pierre Auger Observatory. Our measurement is in agreement with predictions from first-principle calculations.

Acknowledgments.—The successful installation, commissioning, and operation of the Pierre Auger Observatory would not have been possible without the strong commitment and effort from the technical and administrative staff in Malargüe. We are very grateful to the following agencies and organizations for financial support:

Comisión Nacional de Energía Atómica, Agencia Nacional de Promoción Científica y Tecnológica (AN-PCyT), Consejo Nacional de Investigaciones Científicas y Técnicas (CONICET), Gobierno de la Provincia de Mendoza, Municipalidad de Malargüe, NDM Holdings and Valle Las Leñas, in gratitude for their continuing cooperation over land access, Argentina; the Australian Research Council (DP150101622); Conselho Nacional de Desenvolvimento Científico e Tecnológico (CNPq), Financiadora de Estudos e Projetos (FINEP), Fundação de Amparo à Pesquisa do Estado de Rio de Janeiro (FAPERJ), São Paulo Research Foundation (FAPESP) Grants No. 2010/07359-6 and No. 1999/05404-3, Ministério de Ciência e Tecnologia (MCT), Brazil; Grant No. MSMT-CR LG13007, No. 7AMB14AR005, and the Czech Science Foundation Grant No. 14-17501S, Czech Republic; Centre de Calcul IN2P3/CNRS, Centre National de la Recherche Scientifique (CNRS), Conseil Régional Ile-de-France, Département Physique Nucléaire et Corpusculaire (PNC-IN2P3/CNRS), Département Sciences de l’Univers (SDU-INSU/CNRS), Institut Lagrange de Paris (ILP) Grant No. LABEX ANR-10-LABX-63, within the Investissements d’Avenir Programme Grant No. ANR-11-IDEX-0004-02, France; Bundesministerium für Bildung und Forschung (BMBF),

Deutsche Forschungsgemeinschaft (DFG), Finanzministerium Baden-Württemberg, Helmholtz Alliance for Astroparticle Physics (HAP), Helmholtz-Gemeinschaft Deutscher Forschungszentren (HGF), Ministerium für Wissenschaft und Forschung, Nordrhein Westfalen, Ministerium für Wissenschaft, Forschung und Kunst, Baden-Württemberg, Germany; Istituto Nazionale di Fisica Nucleare (INFN), Istituto Nazionale di Astrofisica (INAF), Ministero dell'Istruzione, dell'Università e della Ricerca (MIUR), Gran Sasso Center for Astroparticle Physics (CFA), CETEMPS Center of Excellence, Ministero degli Affari Esteri (MAE), Italy; Consejo Nacional de Ciencia y Tecnología (CONACYT), Mexico; Ministerie van Onderwijs, Cultuur en Wetenschap, Nederlandse Organisatie voor Wetenschappelijk Onderzoek (NWO), Stichting voor Fundamenteel Onderzoek der Materie (FOM), Netherlands; National Centre for Research and Development, Grants No. ERA-NET-ASPERA/01/11 and No. ERA-NET-ASPERA/02/11, National Science Centre, Grants No. 2013/08/M/ST9/00322, No. 2013/08/M/ST9/00728 and No. HARMONIA 5 - 2013/10/M/ST9/00062, Poland; Portuguese national funds and FEDER funds within Programa Operacional Factores de Competitividade through Fundação para a Ciência e a Tecnologia (COMPETE), Portugal; Romanian Authority for Scientific Research ANCS, CNDI-UEFISCDI partnership projects Grants No. 20/2012 and No. 194/2012, Grants No. 1/ASPERA2/2012 ERA-NET, No. PN-II-RU-PD-2011-3-0145-17 and No. PN-II-RU-PD-2011-3-0062, the Minister of National Education, Programme Space Technology and Advanced Research (STAR), Grant No. 83/2013, Romania; Slovenian Research Agency, Slovenia; Comunidad de Madrid, FEDER funds, Ministerio de Educación y Ciencia, Xunta de Galicia, European Community 7th Framework Program, Grant No. FP7-PEOPLE-2012-IEF-328826, Spain; Science and Technology Facilities Council, United Kingdom; Department of Energy, Contracts No. DE-AC02-07CH11359, No. DE-FR02-04ER41300, No. DE-FG02-99ER41107 and No. DE-SC0011689, National Science Foundation, Grant No. 0450696, The Grainger Foundation, USA; NAFOSTED, Vietnam; Marie Curie-IRSES/EPLANET, European Particle Physics Latin American Network, European Union 7th Framework Program, Grant No. PIRSES-2009-GA-246806; and UNESCO.

* auger_spokespersons@fnal.gov

- [1] R. Engel, D. Heck, and T. Pierog, *Ann. Rev. Nucl. Part. S.* **61**, 467 (2011).
- [2] V. Verzi for the Pierre Auger Collaboration, *Proc. 33rd ICRC, Rio de Janeiro, Brazil* (2013).
- [3] P. Abreu *et al.* (Pierre Auger Collaboration), *J. Instrum.* **7**, P09001 (2012).
- [4] J. Abraham *et al.* (Pierre Auger Collaboration), *Astropart. Phys.* **33**, 108 (2010).
- [5] J. Abraham *et al.* (Pierre Auger Collaboration), *Astropart. Phys.* **32**, 89 (2009).
- [6] P. Abreu *et al.* (Pierre Auger Collaboration), *J. Instrum.* **8**, P04009 (2013).
- [7] H. R. Allan, *Progress in Particle and Nuclear Physics: Cosmic Ray Physics* **10**, 169 (1971).
- [8] T. Huege, *Physics Reports* **620**, 1 (2016).
- [9] F. D. Kahn and I. Lerche, *Proc. R. Soc. Lon. Ser. A* **289**, 206 (1966).
- [10] K. Werner and O. Scholten, *Astropart. Phys.* **29**, 393 (2008).
- [11] H. Falcke *et al.* (LOPES Collaboration), *Nature* **435**, 313 (2005).
- [12] C. Glaser for the Pierre Auger Collaboration, *AIP Conf. Proc.* **1535**, 68 (2013).
- [13] W. Apel *et al.* (LOPES Collaboration), *Phys. Rev. D* **90**, 062001 (2014).
- [14] P. A. Bezyazeev *et al.* (Tunka-Rex Collaboration), *Nucl. Instrum. Meth. A* **802**, 89 (2015).
- [15] T. Huege, R. Ulrich, and R. Engel, *Astropart. Phys.* **30**, 96 (2008).
- [16] G. A. Askaryan, *Sov. Phys. JETP* **14**, 441 (1962).
- [17] V. Marin for the Codalema Collaboration, *Proc. 32nd ICRC, Beijing, China* **1**, 291 (2011).
- [18] A. Aab *et al.* (Pierre Auger Collaboration), *Phys. Rev. D* **89**, 052002 (2014).
- [19] M. P. van Haarlem *et al.*, *Astron. Astrophys.* **556**, A2 (2013).
- [20] A. Aab *et al.* (Pierre Auger Collaboration), *Nucl. Instrum. Meth. A* **798**, 172 (2015).
- [21] See Supplemental Material at <http://link.aps.org/supplemental/10.1103/PhysRevLett.116.241101> for a more comprehensive presentation.
- [22] K. Weidenhaupt, *Antenna Calibration and Energy Measurement of Ultra-High Energy Cosmic Rays with the Auger Engineering Radio Array*, Ph.D. thesis, RWTH Aachen University (2014).
- [23] J. Schulz for the Pierre Auger Collaboration, *Proceedings of Science* (2015), 34th ICRC, The Hague, The Netherlands.
- [24] J. Abraham *et al.* (Pierre Auger Collaboration), *Physics Letters B* **685**, 239 (2010).
- [25] A. Aab *et al.* (Pierre Auger Collaboration), *Phys. Rev. D* **93**, 122005 (2016), 1508.04267.
- [26] P. Abreu *et al.* (Pierre Auger Collaboration), *Nucl. Instrum. Meth. A* **635**, 92 (2011).
- [27] P. Abreu *et al.* (Pierre Auger Collaboration), *J. Instrum.* **7**, P10011 (2012).
- [28] A. Nelles *et al.*, *Astropart. Phys.* **60**, 13 (2015).
- [29] K. D. de Vries, A. M. van den Berg, O. Scholten, and K. Werner, *Phys. Rev. Lett.* **107**, 061101 (2011).
- [30] J. Alvarez-Muñiz, W. R. Carvalho, and E. Zas, *Astropart. Phys.* **35**, 325 (2012).
- [31] I. Mariş for the Pierre Auger Collaboration, *Proc. 32nd ICRC, Beijing, China* **1**, 267 (2011).
- [32] D. Ardouin *et al.* (Codalema Collaboration), *Astropart. Phys.* **31**, 192 (2009).
- [33] H. P. Dembinski, B. Kégl, I. C. Mariş, M. Roth, and D. Veberič, *Astropart. Phys.* **73**, 44 (2016).
- [34] D. Ardouin *et al.* (Codalema Collaboration), *Astropart. Phys.* **26**, 341 (2006).
- [35] A. Nelles *et al.*, *J. Cosmol. Astropart. P.* **05**, 018 (2015).

- [36] D. Kostunin *et al.*, *Nucl. Instrum. Meth. A* **742**, 89 (2014), Proc. of 4th Roma Int. Conf. on Astropart. Phys.
- [37] T. Huege, M. Ludwig, and C. W. James, *AIP Conf. Proc.* **1535**, 128 (2013).
- [38] V. Marin and B. Revenu, *Astropart. Phys.* **35**, 733 (2012).